

## Interaction with the S1 $\beta$ -pocket of urokinase: 8-heterocycle substituted and 6,8-disubstituted 2-naphthamidine urokinase inhibitors

Michael D. Wendt,<sup>a,\*</sup> Andrew Geyer,<sup>a</sup> William J. McClellan,<sup>a</sup> Todd W. Rockway,<sup>a</sup>  
Moshe Weitzberg,<sup>a</sup> Xumiao Zhao,<sup>a</sup> Robert Mantei,<sup>a</sup> Kent Stewart,<sup>b</sup>  
Vicki Nienaber,<sup>b</sup> Vered Klinghofer<sup>a</sup> and Vincent L. Giranda<sup>a</sup>

<sup>a</sup>Cancer Research, Global Pharmaceutical R & D, Abbott Laboratories, 100 Abbott Park Road, Abbott Park, IL 60064-6101, USA

<sup>b</sup>Structural Biology, Global Pharmaceutical R & D, Abbott Laboratories, 100 Abbott Park Road, Abbott Park, IL 60064-6101, USA

Received 22 March 2004; revised 12 April 2004; accepted 12 April 2004

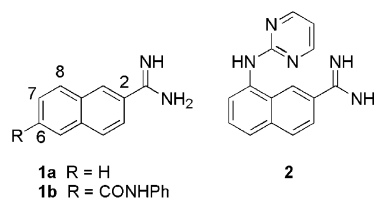
**Abstract**—Several 8-substituted 2-naphthamidine-based inhibitors of the serine protease urokinase plasminogen activator (uPA) are described. Direct attachment of five-membered saturated or unsaturated rings improved inhibitor performance; substitution with sulfones further improved binding profiles. Combination of these substituents or of previously described NH-linked heteroaromatic rings with 6-phenyl amide substituents provided further enhancements to potency and selectivity.

© 2004 Elsevier Ltd. All rights reserved.

Urokinase-type plasminogen activator (uPA), or urokinase, is a trypsin-family serine protease, which is implicated in a variety of tumor-associated processes, including extracellular matrix degradation, invasion, angiogenesis, and metastasis.<sup>1,2</sup> Urokinase converts plasminogen into the active enzyme plasmin, a wide-spectrum protease that digests various components of the extracellular matrix, and also activates proenzymes of matrix metalloproteinases. High levels of urokinase are correlated with enhanced invasiveness and metastasis, and poor prognosis.<sup>2</sup> Additionally, small-molecule urokinase inhibitors of moderate potency have been shown to slow primary tumor growth and metastasis.<sup>3</sup> Consequently, there is great interest in developing more potent and selective inhibitors of urokinase as possible cancer therapeutics.

Previously we described work starting from 2-naphthamidine **1a** including SAR of the 6-phenyl amide **1b**,<sup>4</sup> and 8-position substitution covering NH-linked aromatic rings and carbamates, including X-ray structural studies. The lead compound resulting from the latter

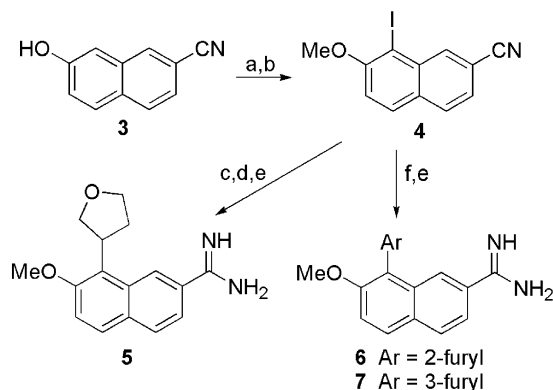
study was the aminopyrimidine **2**.<sup>5</sup> X-ray data suggested that as an alternative to the NH-linked pyrimidine a small ring could be directly attached. Six-membered rings were found to be too large (data not shown), but a small subset of five-membered rings generated a significant increase in binding. Concurrently with that study, 6,8-disubstituted compounds were synthesized in an effort to combine individual binding increments.<sup>6</sup>



Several inhibitors exploring the S1 $\beta$  pocket were synthesized with a methoxy group at the adjacent 7-position. We determined that small groups at the 7-site projected into solvent and had little effect on compound inhibition profiles.<sup>5</sup> Thus, directly linked heterocycles were formed via the iodo compound **4** (Scheme 1), made from the naphthol **3** by regiospecific iodination<sup>7</sup> and methylation. Heck reaction with *cis*-2-butene-1,4-diol gave a cyclic hemiacetal,<sup>8</sup> which was reduced to the

**Keywords:** Urokinase inhibitors.

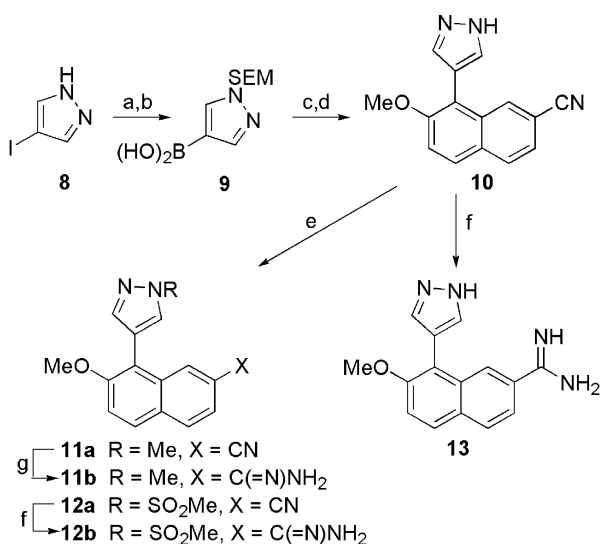
\* Corresponding author. Tel.: +1-847-937-9305; fax: +1-847-935-5165;  
e-mail: [mike.d.wendt@abbott.com](mailto:mike.d.wendt@abbott.com)



**Scheme 1.** Reagents and conditions: (a)  $\text{I}_2$ , aq  $\text{Na}_2\text{CO}_3$ , THF; (b) NaH, MeI, DMF; (c) *cis*-2-butene-1,4-diol,  $\text{PdCl}_2$ ,  $\text{NaHCO}_3$ , NMP,  $130^\circ\text{C}$ , 1 h; (d)  $\text{Et}_3\text{SiH}$ ,  $\text{BF}_3\cdot\text{OEt}_2$ ,  $\text{CH}_2\text{Cl}_2$ ; (e)  $\text{LiN}(\text{TMS})_2$ , THF, then 1 M HCl; (f) 2- or 3-furylboronic acid,  $\text{Pd}(\text{OAc})_2$ , dppf,  $\text{Cs}_2\text{CO}_3$ , DMF.

tetrahydrofuran and converted to the amidine **5** using the  $\text{LiN}(\text{TMS})_2$  amidination protocol.<sup>9</sup> Suzuki couplings followed by  $\text{LiN}(\text{TMS})_2$  amidination gave **6** and **7**. Pyrazoles (Scheme 2) were made by first synthesizing the SEM-protected boronic acid **9** via transmetalation of **8** and trapping with  $\text{B}(\text{OMe})_3$ , and protection. Suzuki coupling to **4** and deprotection gave **10**, which was alkylated and sulfonylated through its potassium anion in DMF. Amidines **12b** and **13** were made via the thioamide,<sup>10</sup> while the  $\text{LiN}(\text{TMS})_2$  method was used for **11b**.

6,8-Disubstituted compounds were made beginning with the known cyanoester **14** (Scheme 3). Bromination at the 8-position proceeded cleanly using 1,3-dibromo-5,5-dimethylhydantoin.<sup>11</sup> The resulting ester was saponified, converted to the acid chloride, and reacted with the appropriate anilines<sup>12</sup> to give **15a–c**. A repeat of the



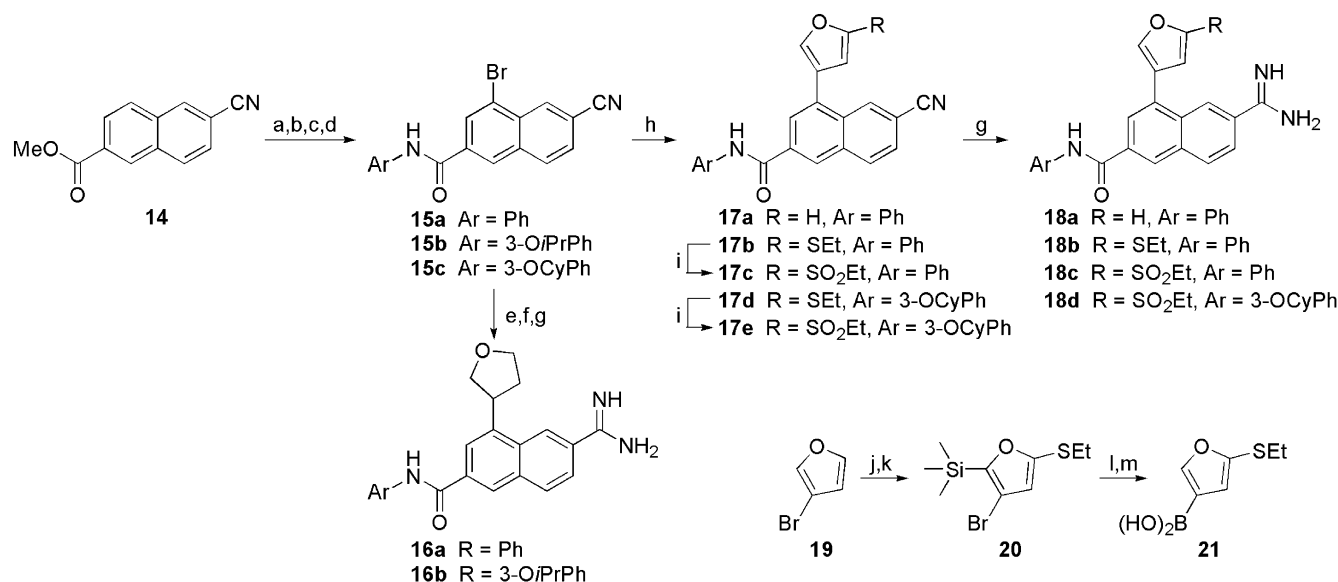
**Scheme 2.** Reagents and conditions: (a) NaH, SEMCl, DMF; (b) BuLi,  $\text{B}(\text{OMe})_3$ , then 1 M HCl; (c) **4**,  $\text{PdCl}_2$  (dppf),  $\text{Cs}_2\text{CO}_3$ , DMF; (d) TBAF, THF,  $\Delta$ ; (e) RX, KHMDS, DMF; (f)  $\text{H}_2\text{S}$ , TEA, pyridine, then MeI, acetone, then  $\text{NH}_4\text{OAc}$ , MeOH; (g)  $\text{LiN}(\text{TMS})_2$ , THF, then 1 M HCl.

tetrahydrofuran-forming reactions and amidination gave **16a,b**, while Suzuki reactions led to **17a,b,d**. Oxidation to the sulfones **17c,e** was easily carried out with *m*CPBA, and the furan-containing nitriles were again carried on to amidines. The syntheses of furans **17b,d** required the functionalized boronic acid **21**, which was made from **19** by a blocking/deblocking strategy employing a TMS group. 8-Aminopyrimidines were installed by nitration of **14**, followed by reduction to the amino compound and Pd-catalyzed amine coupling to 2-bromopyrimidine. The resulting ester **22** was then saponified and coupled to anilines<sup>12</sup> to give amidonitriles, which were converted via thioamides to the amidines **23a,b** (Scheme 4).

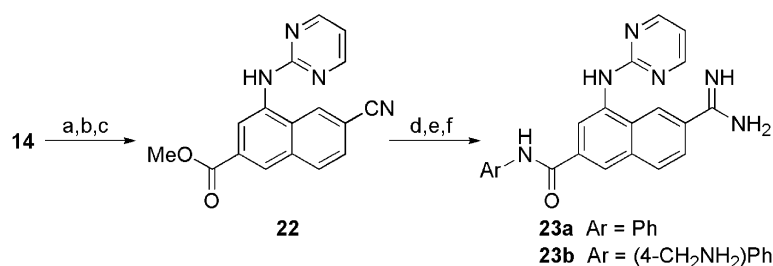
We expected positions on heterocyclic rings adjacent to the connecting bond to be buried by protein; consequently we felt heteroatoms would be best deployed at the more solvent exposed positions. This was immediately borne out by the furans **6** and **7**. In Table 1, binding data is shown for urokinase and a representative panel of trypsin-like serine proteases involved in coagulation and proteolysis. The 3-furyl **7** picks up a larger increment of binding than does the 2-furyl **6**. Further, the 3-tetrahydrofuran **5** also improves affinity to uPA. We found saturated rings attached by an NH group, analogous to the aminopyrimidines reported earlier, to bind very poorly to uPA (data not shown), but the 3-THF series in all cases bound with nearly identical affinities to uPA and the other trypsin-like serine proteases compared to corresponding 3-furans. Neither **5** nor **7**, however, are more selective regarding the panel in general than **1a**. When combined with phenyl amides at position 6, as in **16a** and **18a**, these substituents contribute affinity increases in roughly additive fashion to yield double-digit nanomolar compounds against uPA. As the phenyl amide **1b** also fails to impart a selectivity advantage over **1a** on its own, **16a** and **18a** likewise maintain similar selectivity profiles to those of **5** and **7**. **16b**, however, possesses the additional isopropoxy group, which interacts with the previously described hydrophobic ‘dimple’ region of uPA.<sup>4</sup> Thus **16b** displays improved selectivity, particularly against kallikrein and thrombin. Moreover, **16b** achieves single-digit activity against uPA.

Additional heterocycles were studied; the pyrazole series offered a solvent exposed heteroatom and a second nitrogen atom easily amenable to substitution. Though the parent pyrazole **13** and compounds with N-alkyl substituents such as **11b** offer no improvement over **1a**, the N-methylsulfonyl **12b** produces not only improved binding to uPA but also a small increase in selectivity against the entire panel of serine proteases.

We next sought to combine the two incremental improvements found, in the form of alkylsulfonylfurans. The 3-furan **7** itself is threefold more potent than the pyrazole, and substituent additivities seemed to hold for alkylsulfonylfurans. When combined with phenyl amide substituents at position 6, **18c** and its immediate synthetic precursor **18b** again display greatly enhanced binding to uPA, with **18c** fivefold more potent than the



**Scheme 3.** Reagents and conditions: (a) DBMH, TfOH, CH<sub>2</sub>Cl<sub>2</sub>; (b) LiOH, THF, MeOH, H<sub>2</sub>O; (c) (COCl)<sub>2</sub>, toluene, 55 °C; (d) aniline, toluene; (e) *cis*-2-butene-1,4-diol, PdCl<sub>2</sub>, NaHCO<sub>3</sub>, NMP, 130 °C, 1 h; (f) Et<sub>3</sub>SiH, BF<sub>3</sub>·OEt<sub>2</sub>, CH<sub>2</sub>Cl<sub>2</sub>; (g) LiN(TMS)<sub>2</sub>, THF, then 1 M HCl; (h) **21** or furan-3-boronic acid, PdCl<sub>2</sub> dppf, Cs<sub>2</sub>CO<sub>3</sub>, DMF, 90 °C; (i) *m*CPBA, CH<sub>2</sub>Cl<sub>2</sub>; (j) LDA, TMSCl, THF, −78 °C; (k) LDA, EtSSEt, THF, −78 °C; (l) TBAF, THF; (m) BuLi, B(OMe)<sub>3</sub>, THF, −78 °C, then 1 M HCl.



**Scheme 4.** Reagents and conditions: (a) KNO<sub>3</sub>, H<sub>2</sub>SO<sub>4</sub>, 0 °C; (b) H<sub>2</sub>, 10% Pd/C, EtOAc, THF; (c) 2-bromopyrimidine, Pd/dba<sub>3</sub>, BINAP, NaO-*t*-Bu, toluene, 80 °C; (d) LiOH, THF, MeOH, H<sub>2</sub>O; (e) aniline, HATU, DIPEA, DMF; (f) H<sub>2</sub>S, TEA, pyridine, then MeI, acetone, then NH<sub>4</sub>OAc, MeOH.

unsubstituted furan **18a**, but both **18b** and **18c** fail to completely reproduce the improvements in selectivity seen with **12b**. While comparison of **13** and **12b**, and **18a** and **18c**, indicate that the methylsulfonyl group is responsible for a fourfold boost in affinity, it may be that the pyrazole is more selective than the other heterocycles, and imparts the slight increase in selectivity seen for **12b**. Finally, the cyclopentyloxy-appended **18d** generates improved selectivity across the panel, and was 2 nM against uPA.

In spite of the gains made in the binding profile of our inhibitors by appending heterocycles at the 8-position, the series of NH-linked heterocycles, in particular the aminopyrimidine, nevertheless generates greater affinity and far greater selectivity improvements to the naphthamidine scaffold. Compound **2**, possessing no 6-substituent, possesses better overall selectivity than **12b**, and is 18-fold more active against uPA. Addition of a simple phenyl amide, resulting in **23a**, brings the overall profile to a level similar to **18d**. Further addition of alkoxy groups to the phenyl amide improves the binding profile in a similar manner to the examples above (data not

shown), however the compound with the best overall profile is **23b**, resulting from addition of a *para*-amino-methyl group to the phenyl amide.<sup>4</sup>

Structural aspects of the binding of inhibitors with 8-heterocycle substitution are exemplified by the co-crystal of **12b** and uPA.<sup>13</sup> The periphery of the S1β pocket is defined by residues Gln192, Lys143, Ser146, and Gly218, while the Cys191-Cys220 disulfide linkage helps form the base of the subsite. Figure 1a shows the X-ray structure of **12b** bound to uPA, with the methylsulfonylpyrazole effectively filling the S1β pocket. The methyl group extends into the farthest region of the S1β pocket, with the oxygen atoms extended toward solvent. Superimposed on **12b** in Figure 1b is compound **2**, with the aminopyrimidine also efficiently filling the S1β pocket.<sup>5</sup> Amino acid residues in the vicinity of the inhibitors are essentially identical for both X-ray structures, with the exception of Gly216 (Fig. 1b), which with **2** is angled toward the bridging NH, with a hydrogen bond distance of 3.4 Å. Previous work showed that this NH group, present in a variety of substituents, is uniformly worth close to 1.5 kcal/mol, or about a 13-fold

**Table 1.** Inhibition profiles of 8- and 6,8-substituted 2-naphthamidines

Compound	Substituent			$K_i$ ( $\mu\text{M}$ ) <sup>a</sup>					
	6	7	8	uPA	P-Kall	tPA	Trypsin	Plasmin	Thrombin
<b>1a</b>				5.9	23	>100	7.8	51	—
<b>1b</b>	Ph			0.63 (0.09)	2.5 (1.1) <sup>b</sup>	32 (18) <sup>b</sup>	0.33 (0.18) <sup>c</sup>	2.0 (0.6) <sup>b</sup>	5.6 (2.2) <sup>b</sup>
<b>5</b>		OMe		0.53	3.3	7.4	0.32	6.0	0.45
<b>6</b>		OMe		2.1					
<b>7</b>		OMe		0.82	3.7	18	1.2	9.4	1.3
<b>13</b>		OMe		2.3					
<b>11b</b>		OMe		4.6					
<b>12b</b>		OMe		0.63	14	>100	2.7	8.5	7.1
<b>16a</b>	Ph			0.106 (.013)	0.40	0.87	0.03	0.40	0.36
<b>16b</b>				0.0085 (.0007)	0.30	0.13	0.012	0.19	1.1
<b>18a</b>	Ph			0.091 (0.011)	0.27	0.18	0.045	0.32	0.13
<b>18b</b>	Ph			0.040 (0.004)	0.069	3.3	0.011	0.053	0.12
<b>18c</b>	Ph			0.018 (0.004)	0.019	8.3	0.0035	0.056	0.29
<b>18d</b>				0.0021 (0.0002)	0.07	1.6	0.003	0.038	0.61
<b>2</b>				0.035 (0.007)	1.0 (0.5)	24 (17)	1.7 (0.2)	3.8 (1.1)	3.2 (1.1)
<b>24</b>				0.45	1.9	27	0.2	6.6	5.2
<b>23a</b>	Ph			0.0020	0.10	0.81	0.04	0.09	0.17
<b>23b</b>				0.00062 (0.00005)	0.04	0.68	0.02	0.15	0.94

<sup>a</sup> Values are means of three experiments. Values in parentheses are standard deviations of two separate measurements, except where noted.<sup>b</sup> Nine measurements.<sup>c</sup> Eight measurements.

improvement in affinity, leaving another 10-fold improvement, or 1.4 kcal/mol to be attributed to the pyrimidine ring.<sup>5</sup> The sulfonylpyrazole itself also results in about a 10-fold improvement; thus it may appear that, absent more specific interactions, this is roughly the affinity gain expected from filling the S1 $\beta$  subsite of uPA.

Selectivity gains from the aminopyrimidine of **2** seem to come mostly from the pyrimidine ring itself, as seen by comparison with the amino compound **24**.<sup>5</sup> Given the conserved nature of Gly216, and the highly variable identities of the S1 $\beta$ -forming residues 143 and 146 among the other proteases, it seems reasonable to assume that the gain in binding for **2** results from a good

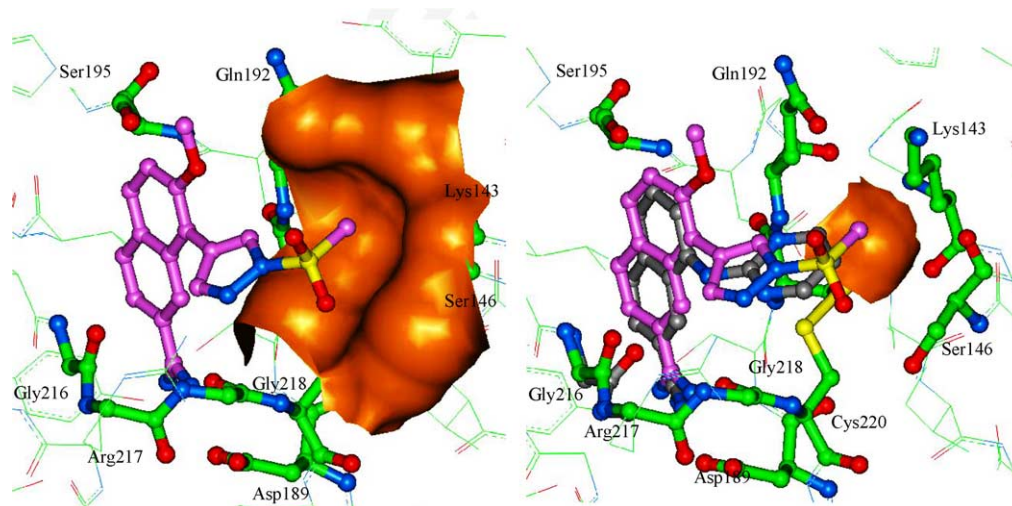


**Figure 1.** (a) Compound **12b** and surface of S1 $\beta$  pocket with key residues highlighted and labeled; (b) **12b** and **2** with surface of S1 $\beta$  pocket cut away to allow view of pocket-forming residues. Compound **2** and the corresponding location of Gly216 are overlaid in gray. Other protein residues in the structure with **2** have an near-identical orientation to that with **12b**. Unlabeled Cys191 is behind the 8-substituent groups.

fit of the ring with the S1 $\beta$  pocket of uPA, whereas the fit with corresponding regions of other proteases neither adds to nor subtracts from affinity. Only trypsin suffers a drop in affinity to **2** due to the pyrimidine, probably resulting from an asparagine substitution for Lys143.

However, while the overlap of the 8-substituents of **12b** and **2** in Figure 1b is substantial, the selectivities imparted by the methylsulfonylpyrazole of **12b**, or by the ethylthiofuran of **18b** or the ethylsulfonylfuran of **18c**, do not follow the pattern set by **2**. Again, the direct-linked heterocycles themselves seem to impart little or no selectivity, while the alkylsulfonyl group only seems to impact the affinity toward tPA. In the S1 $\beta$ -forming region, tPA is particularly similar to uPA, differing only in possessing an Ala146 rather than a serine. It is important to note that the backbone structures of all the proteins are similar to uPA in this region. This is particularly so for tPA, thus it is difficult to rationalize the decrease in affinity to tPA upon appending an alkylsulfonyl group or even an alkylthio group to an 8-heterocycle. We note that there appears to be a weak hydrogen bond between the Ser146 hydroxyl group of uPA and a sulfonyl oxygen with a distance of 3.2 Å, but this interaction is missing for all of the other serine proteases, and not just tPA. Thus, it seems evident that selectivity changes in this region depend on more subtle factors.

A last point relating to binding in Figure 1b is the orientation of the inhibitor cores. Throughout our studies, we assumed that substituent effects at the 6- and 8-positions would be additive, and further, that individual segments of a single substituent would have similarly additive effects. Our binding data confirmed this to within experimental error; more convincingly, our collected X-ray structures attest to the substantial invariance of inhibitor binding conformations. A further illustration is shown as Figure 2, where the crystal structures of **1b** and **23b** bound to uPA are superimposed.

In general, we saw only rotations of the naphthyl group of a few degrees, and translations within the S1 subsite toward or away from Asp189 of no more than a few tenths of an Ångström. Further, these movements did not appear to be systematically related to any substituent type.

In summary, a new group of uPA inhibitors have been developed by combining structural units interacting with the S1 $\beta$  pocket and additional subsites described in detail earlier. These interactions, illustrated by a wealth of structural information, are substantially additive in nature, and have resulted in selective and extremely potent inhibitors and an increased understanding of

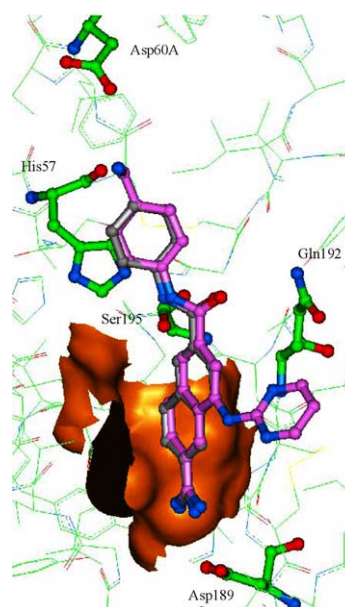


**Figure 2.** Compound **1b** (gray) and **23b** (pink) overlaid. H57, D60, D189, Q192, and S195 are shown in thick bonds. The surface of the S1 pocket is shown.

how to exploit the uPA structure to design still more effective inhibitors.

### References and notes

1. (a) Rabbani, S. A.; Xing, R. H. *J. Int. Oncol.* **1998**, *12*, 911; (b) Bell, W. R. *Sem. Thromb. Hemost.* **1996**, *22*, 459; (c) Blasi, F. *APMIS* **1999**, *107*, 96.
2. (a) Andreasen, P. A.; Kjoller, L.; Christensen, L.; Duffy, M. J. *Int. J. Cancer* **1997**, *72*, 1; (b) Achbarou, A.; Kaiser, S.; Tremblay, G.; Sainte-Marie, L. G.; Brodt, P.; Goltzman, D.; Rabbani, S. A. *Cancer Res.* **1994**, *54*, 2372; (c) Duffy, M. J. *Biochem. Soc. Trans.* **2002**, *30*, 207.
3. (a) Evans, D.; Sloan-Stakleff, K.; Arvan, M.; Guyton, D. *Clin. Exp. Metastasis* **1998**, *16*, 353; (b) Rabbani, S.; Harakidas, P.; Davidson, D.; Henkin, J.; Mazar, A. *Int. J. Cancer* **1995**, *63*, 840; (c) Alonso, D. F.; Tejera, A. M.; Farias, E. F.; Bal de Kier Joffe, E.; Bomez, D. E. *Anticancer Res.* **1998**, *18*, 4499; (d) Xing, R. H.; Mazar, A.; Henkin, J.; Rabbani, S. A. *Cancer Res.* **1997**, *57*, 3585.
4. Wendt, M. D.; Rockway, T. R.; Geyer, A.; McClellan, W.; Weitzberg, M.; Zhao, X.; Mantei, R.; Nienaber, V. L.; Stewart, K.; Klinghofer, V.; Giranda, V. L. *J. Med. Chem.* **2004**, *47*, 303.
5. Nienaber, V. L.; Davidson, D.; Edalji, R.; Giranda, V. L.; Klinghofer, V.; Henkin, J.; Magdalinos, P.; Mantei, R.; Merrick, S.; Severin, J. M.; Smith, R. A.; Stewart, K.; Walter, K.; Wang, J.; Wendt, M.; Weitzberg, M.; Zhao, X.; Rockway, T. *Structure* **2000**, *8*, 553.
6. (a) Rockway, T. W.; Nienaber, V.; Giranda, V. L. *Curr. Pharm. Des.* **2002**, *8*, 2541; (b) Rockway, T. W.; Giranda, V. L. *Curr. Pharm. Des.* **2003**, *9*, 639.
7. Edgar, K. J.; Falling, S. N. *J. Org. Chem.* **1990**, *55*, 5287.
8. Chalk, A. J.; Magennis, S. A. *J. Org. Chem.* **1976**, *41*, 273.
9. Boere, R. T.; Oakley, R. T.; Reed, R. W. *J. Orgmet. Chem.* **1987**, *331*, 161.
10. Brederbeck, H.; Gompper, R.; Seiz, H. *Chem. Ber.* **1957**, *90*, 1837.
11. Eguchi, H.; Kawaguchi, H.; Yoshinaga, S.; Nishida, A.; Nishiguchi, T.; Fujisaki, S. *Bull. Chem. Soc. Jpn.* **1994**, *67*, 1918.
12. Substituted aniline syntheses were reported in Ref. 4.
13. Crystallographic data for structures are on file with CCDC. Deposition numbers: **1b**, 1OWE; **2**, 1SQO; **12b**, 1SQT; **23b**, 1SQA.